Embryonic thermosensitive TRPA1 determines transgenerational diapause phenotype of the silkworm, *Bombyx mori*

Azusa Sato[1]*, Takaaki Sokabe[2]*, Makiko Kashio[2], Yuji Yasukochi[3], Makoto Tominaga[2, 4], Kunihiro Shiomi[1‡]

[1]Faculty of Textile Science and Technology, Shinshu University, Ueda 386-8567, Japan
[2]Division of Cell Signaling, Okazaki Institute for Integrative Bioscience (National Institute for Physiological Sciences), National Institutes of Natural Sciences, Okazaki 444-8787, Japan
[3]National Institute of Agrobiological Sciences (NIAS), Tsukuba 305-8602, Japan
[4]Department of Physiological Sciences, The Graduate University for Advanced Studies, Okazaki 444-8585, Japan
*These two authors contributed equally to this work.
‡Address correspondence to: K. Shiomi, Faculty of Textile Science and Technology, Shinshu University, Ueda, Nagano, 386-8567, Japan, Tel: +81-268-21-5338; Fax: +81-268-21-5331; E-mail: shiomi@shinshu-u.ac.jp

Abbreviations: 25DD, silkworm incubated at 25°C under continuous darkness during maternal embryogenesis; 15DD, silkworm incubated at 15°C under continuous darkness during maternal embryogenesis; CA, cinnamaldehyde; CNS, central nervous system; DAPI, 4,6-diamidino-2-phenylindole; DH, diapause hormone; DHPCs, DH-PBAN-producing neurosecretory cells; dsRNA, double-stranded RNA; DW, distilled water; EGFP, enhanced green fluorescent protein; FXPRLa, phe-X-Pro-Arg-Leu-NH_2; ILPs, insulin-like peptides; ORF, open reading frame; PBAN, pheromone-biosynthesis-activating neuropeptide; PBS, phosphate-buffered saline; PCR, polymerase chain reaction; RNAi, RNA interference; RT-PCR, reverse transcription-PCR; SEM, scanning electron microscope; SG, subesophageal ganglion; SLb, labial neuromere cell of the SG; TRP, transient receptor potential.

Running title: Thermosensitive TRPA1 of *Bombyx*

Abstract

In the bivoltine strain of the silkworm, *Bombyx mori*, embryonic diapause is induced transgenerationally as a maternal effect. Progeny diapause is determined by the environmental temperature during embryonic development of the mother; however, its molecular mechanisms are largely unknown. Here, we show that the *Bombyx* TRPA1 ortholog (*BmTrpA1*) acts as a thermosensitive transient receptor potential (TRP) channel that is activated at temperatures above ~21°C and affects the induction of diapause in progeny. In addition, we show that embryonic RNAi of *BmTrpA1* affects diapause hormone release during pupal-adult development. This is the first study to identify a thermosensitive TRP channel that acts as a molecular switch for a relatively long-term predictive adaptive response by inducing an alternative phenotype to seasonal polyphenism.

Key words: diapause hormone, transient receptor potential, thermosensitive TRP channel, seasonal polyphenism

Significance Statement

Diapause has evolved as a specific subtype of dormancy in most insect species and as a seasonal polyphenism that ensures survival under unfavorable environmental conditions and synchronizes populations. In *Bombyx mori*, embryonic diapause is induced transgenerationally as a maternal effect. However, the molecular mechanisms involved in the perception of environmental temperature and in linking thermal information to neuroendocrine functions are still unknown. Here, we show that the *Bombyx* TRPA1 could be thermally activated during embryogenesis, and an unknown signaling pathway linked to the release of diapause hormone may then be activated to affect the induction of diapause in progeny. The *Bombyx* TRPA1 acts as a molecular switch for the development of an alternative phenotype in an animal with seasonal polyphenism.

\body

Seasonal polyphenism is the differential expression of alternative phenotypes from a single genotype, depending upon environmental conditions such as photoperiod, temperature, and nutrition (1, 2). This differential expression is a form of developmental phenotypic plasticity that evolved for seasonal adaptation. In some cases, this type of environmental response improves fitness at a later stage of development, or of progeny more distant than the next generation. This is known as a predictive adaptive response and is matched to the environment predicted to be experienced at a later phase in the organism's life history (3, 4). However, the molecular basis for seasonal polyphenism is largely unknown.

Diapause is a type of seasonal polyphenism and represents one of the most dramatic developmental switches that has been described in the field of biology. Diapause has evolved as a specific subtype of dormancy in most insect species that ensures survival under unfavorable environmental conditions and that synchronizes populations (5). In many insects, environmental cues that signal future environmental changes induce the development of alternative seasonal phenotypes. These alternative phenotypes are accompanied by changes in energy metabolism or storage to improve cold/stress tolerance in later life-history stages or in progeny (6, 7). In populations of *Bombyx mori* that have two generations per year, embryonic diapause is induced transgenerationally as a maternal effect (Fig. 1a). Progeny diapause is determined by the environmental temperature during embryonic development of the mother. When eggs are incubated at 25°C under continuous darkness, the resultant female moths (25DD) lay diapause eggs. In contrast, incubation of eggs at 15°C in dark condition results in moths (15DD) that lay non-diapause eggs (8, 9). While non-diapause eggs complete

their embryogenesis 10 days after oviposition at 25°C, diapause eggs remain dormant until exposed to appropriate diapause-breaking conditions. For example, exposure of diapause eggs to a temperature as low as 5°C for over 60 days completely terminates diapause, and when transferred to 25°C, the eggs resume embryogenesis (10). The diapause/non-diapause phenotype is determined only during a sensitive period. This period lasts for 3 days in 25DD or for 9 days in 15DD and corresponds to stages 20–23 of embryogenesis (see Fig. 2a). Transient incubation, or incubation for only part of the sensitive period, of eggs at 25°C or 15°C never results in eggs that are uniformly diapause or non-diapause (8, 11). Thus, the diapause of *B. mori* progeny can be controlled by changing the environmental temperature during the sensitive period of embryonic development, but the temperature must continuously remain in the appropriate range for a relatively long and restrictive period.

At the molecular level, diapause in *B. mori* is regulated hormonally by diapause hormone (DH), a member of the FXPRLa neuropeptide family that is responsible for diapause induction. DH acts on a G-protein-coupled receptor in the developing ovaries of females during pupal-adult development (12, 13) and is produced in DH-pheromone-biosynthesis-activating neuropeptide (PBAN)-producing neurosecretory cells (DHPCs) located within the subesophageal ganglion (SG) (14-16). DH levels in the SG and SG-brain complex are markedly lower in 25DD pupae than in 15DD pupae, although level of mRNA expression is higher in 25DD than in the 15DD pupae at the early to middle stages of pupal-adult development (11, 17). The labial neuromere cell of the SG (SLb) somata are DHPCs, and transport of DH from the SLb somata is actively modified in response to temperature and light conditions during the embryonic development of 25DD pupae. These changes can result in active release of

DH into the hemolymph during the middle pupal stages, during which the developing ovaries are sensitive to DH (12, 16). Thus, environmental thermal information is stored for a long time period (approximately one month) until the middle pupal stage, and is transduced to neuroendocrine signals (DH release) to induce progeny diapause. However, the molecular mechanisms involved in perception of environmental temperature and in linking thermal information to neuroendocrine functions are still unknown.

Thermosensitive transient receptor potential (TRP) channels are key players in thermal sensation in both vertebrate and invertebrate organisms (18-21). In insects, TRPA1 and other TRPA subtypes mediate the sensing of increases in temperature. One such TRPA, *Drosophila* TRPA1, is activated at a threshold of ~27°C and regulates thermotaxis (22-24). Furthermore, it has been reported that other *Drosophila* TRP channels are involved in cold sensation and cold-avoidance behavior (25, 26). *Anopheles* TRPA1 is activated by temperature increases from 25°C to ~37°C, and it is hypothesized that this activation allows insects to detect increasing temperature gradients derived from host body heat during crucial, close-range host-seeking behaviors (27). Another TRPA subfamily member, AmHsTRPA, is activated in honeybees at a threshold of 34°C. It has been proposed that AmHsTRPA mediates detection of brood nest temperatures >36°C and induces nest-cooling behavior (28). Therefore, in insects, the thermosensitive TRPA channels are involved in the detection of, and the short-term and immediate response to, extreme variability in temperature.

Here, we report that a *Bombyx* TRPA1 (BmTRPA1) ortholog acts as a thermosensitive TRP channel that is activated at a threshold of ~21°C and determines progeny diapause during maternal embryonic development. This is the first report of a

thermosensitive TRP channel that acts as a molecular switch for a relatively long-term predictive adaptive response by inducing an alternative phenotype to seasonal polyphenism, but that does not result in an immediate organismal response.

Results

Embryonic *BmTrpA1* is involved in progeny diapause induction

Consistent with previous reports (29), we found genes for 13 TRP channel superfamily members in the *Bombyx* genome. We successfully cloned the full-length cDNA of five TRPA subfamily genes, *BmTrpA1*, *BmPainless*, *BmPyrexia*, *BmWtrw*, and *BmTrpA4*, using a PCR-based strategy. We then evaluated the effects of RNAi on progeny embryos to determine whether any of these *Bombyx* TRPA subfamily members were involved in diapause induction. To accomplish this, each double-stranded RNA (dsRNA) corresponding to the *Bombyx TrpA* subfamily genes was injected into newly laid non-diapause eggs, and the eggs were incubated at 25°C during embryogenesis. The eclosed moths were allowed to oviposit, and the percentages of non-diapause eggs were determined (25DD, Fig. 1b). We predicted that the TRP channel would be important in progeny diapause induction; this would be demonstrated if non-diapause eggs were laid by 25DD dsRNA-injected moths. While 15DD and 25DD moths laid all non-diapause or all diapause eggs respectively, injection of one dsRNA sequence that corresponded to *BmTrpA1* and incubation at 25°C resulted in non-diapause eggs in the next generation (25DD, 9.7 ± 26.1%, Fig. 1b; and Supplementary Fig. S1a). Similarly, injection of another dsRNA sequence corresponding to *BmTrpA1* also resulted in the development of non-diapause eggs (4.5 ± 15.6%, Supplementary Figs. S1b and S2a). Few or no non-diapause eggs developed after injection of phosphate-buffered saline (PBS), the dsRNA corresponding to *EGFP,* or the dsRNA corresponding to other *TrpA* family genes (Fig. 1b and Supplementary Figs. S1a and S2a). Furthermore, the non-diapause-type was not disrupted by injection of dsRNA corresponding to *BmTrpA1* and incubation at 15°C (15DD, Fig. 1b; Supplementary Fig. S1a). We confirmed that

both of the dsRNAs corresponding to *BmTrpA1* strongly suppressed the level of *BmTrpA1* mRNA (Supplementary Fig. S2b), and observed that *BmTrpA1* RNAi affected the duration of larval development (Fig. 1c). Generally, 15DD larvae initiate spinning earlier than 25DD larvae, as indicated in Fig. 1c. The peak of spinning initiation for 15DD larvae occurred 18 d (AM) after hatching. However, the 25DD larvae initiated spinning 20 d (PM) after hatching and the peak occurred at 22 d (AM). *BmTrpA1* larvae exhibited two peaks in spinning initiation (Fig. 1c, *trpA1*). Interestingly, larvae that initiated spinning at 19 d oviposited non-diapause eggs (35.3 ± 40.2%), whereas larvae that initiated spinning at 20–23 d did not lay any non-diapause eggs (Fig. 1b and c). *EGFP* injection did not affect initiation of spinning. These results suggest that embryonic *BmTrpA1* is involved in both progeny diapause induction and the duration of larval development.

Developmental expression profile of BmTRPA1 during embryogenesis

We examined the expression of *BmTrpA1* during the embryonic development of eggs incubated at 25DD or 15DD using reverse transcription polymerase chain reaction (RT-PCR) analysis. *BmTrpA1* mRNA was slightly expressed during early embryonic stages and increased during the middle embryonic stages, including the sensitive periods, under both temperature conditions (Fig. 2a, lanes 8–12 and 46–50). We then examined the distribution of *BmTrpA1* mRNA in eggs during developmental stage (st.) 21, which is the sensitive period (Fig. 2e). Scanning electron microscope (SEM) observations indicated that differentiation and histogenesis of larval tissues occurs during st. 20–23 and the head and thorax of the embryo become distinguishable after st. 20 (Fig. 2b). Blastokinesis then proceeds actively, and dorsal closure is

completed during st. 21 (Fig. 2c). During st. 22, complete embryonic reversal occurs and trichogenous cell masses appear in st. 23 (Fig. 2d). Expression of *BmTrpA1* was predominantly detected in mRNA derived from a mixture of thoracic and abdominal tissues (Fig. 2e, lane 4).

We subsequently examined the developmental profiles and localization of BmTRPA1 by using the anti-BmTRPA1 antibody. First, we performed immunostaining on HEK293 cells transfected with *BmTrpA1* to confirm the immunoreactivity of anti-BmTRPA1 (Supplementary Fig. S3a–c). Then, using Western blot analysis, the immunoreactive bands were detected at ~130 kDa in 4.0, 5.5, and 9.0 d, including the sensitive periods after oviposition (Supplementary Fig. S3d, lanes 1–4; arrow). These bands were similar to the predicted molecular weight of BmTRPA1 (131.363 Da), suggesting that they were derived from BmTRPA1. Furthermore, the intensity of these bands was lower in dsRNA-injected embryos (Supplementary Fig. S3d, lanes 5, 6), suggesting that RNAi of *BmTrpA1* was effective for decreasing BmTRPA1 accumulation and that the anti-BmTRPA1 antibody recognized BmTRPA1 in embryos. We examined the localization of BmTRPA1 in embryogenesis by whole-mount immunohistochemistry (Fig. 2f–k). With advancing embryogenesis, immunoreactive signals were first detected in the ventral surface of the caudal portion of the embryo in st. 20 (Fig. 2f), and intensive signals were detected in both sides of the tips of anal prolegs in st. 23 (Fig. 2i). In addition, intensive signals were detected in the tips of prolegs during sts. 21 and 23 (Fig. 2g–h and j respectively). In a single section with DAPI staining, immunoreactive signals were clearly detected in the epidermal surfaces of proleg tips (Fig. 2h, arrowheads). Furthermore, immunoreactive signals were observed in st. 23 trichogenous tormogen cells that formed the bristle sockets (Fig. 2k).

To confirm the specificity of immunoreactive signals in embryos, we compared the intensity of the signals to dsRNA-injected embryos (Supplementary Fig. S3e–l). Immunoreactive signals disappeared or decreased in RNAi embryos. Thus, BmTRPA1 is predominantly and ubiquitously localized in the epidermal non-neural cells of various tissues.

BmTrpA1 RNAi affects immunoreactivity of DH in pupal neurosecretory cells

Immunohistochemistry using anti-DH antibody on pupae after 4 d of pupation indicated that, in a pair of SLb somata, one of the DHPCs of the SG in pupae (25DD) injected with PBS had lower DH immunoreactivity (30.2 ± 22.2%) than those of SLb somata from 15DD pupae (Fig. 3a–b and e). As described previously (16), this indicates that DH is actively released from these neurosecretory cells in 25DD pupae and that its activity is closely correlated with the determination of diapause type. If BmTRPA1 indeed affects diapause status in progeny through control of DH release, it is predicted that the immunoreactive intensity of SLb cells would be altered by RNAi. DH immunoreactivity was similar in *BmTrpA1* RNAi of 25DD and 15DD pupae (93.7 ± 24.4%; Fig. 3c and e). On the other hand, injection of *EGFP* dsRNA resulted in immunoreactive intensity that was similar to that of PBS-injected (25DD) pupae (35.3 ± 36.6%; Fig. 3d and e). These results suggest that embryonic *BmTrpA1* RNAi affects DH release during pupal-adult development.

BmTRPA1 is a thermosensitive TRP channel activated above 21°C

To examine whether BmTRPA1 is a thermosensitive TRP channel, we first performed Ca^{2+}-imaging experiments using fura-2 to determine whether

BmTRPA1-expressing cells increased intracellular Ca^{2+} concentration ($[Ca^{2+}]_i$) upon temperature fluctuation (Fig. 4a). There was no change in $[Ca^{2+}]_i$ when temperature was reduced from 25°C to 15°C, but a clear increase in $[Ca^{2+}]_i$ was observed in BmTRPA1-expressing cells when the temperature was raised to >25°C (Fig. 4a and b). However, the $[Ca^{2+}]_i$ increase was abolished in the absence of extracellular Ca^{2+} (Supplementary Fig. S4a), indicating that it was caused by an influx of Ca^{2+} from the extracellular space through BmTRPA1. Next, we conducted patch-clamp experiments to clarify the electrophysiological properties of BmTRPA1. In the whole-cell configuration, BmTRPA1-expressing cells showed transient inward currents at membrane potential of –60 mV when the temperature was increased from 15°C to >20°C, but not when it was decreased from 25°C (Fig. 4c). Mock-transfected HEK293 cells did not display heat-induced $[Ca^{2+}]_i$ increases in a Ca^{2+}-imaging experiment (Supplementary Fig. S4b), suggesting that the currents are specifically mediated through BmTRPA1. A temperature profile of BmTRPA1 activation showed that the current gradually began to develop at temperatures >21°C, followed by large transient currents toward 40°C (Fig. 4c and d). An Arrhenius plot showed a flex point at 21.6 ± 1.8°C, and the mean Q_{10} value was markedly shifted at this temperature, from 1.7 ± 0.3 to 20.5 ± 5.6 (Fig. 4e). These values are comparable to those of known thermosensitive TRP channels (30). We therefore conclude that BmTRPA1 is a temperature-sensitive ion channel activated at temperatures >21°C.

BmTRPA1 is activated by chemical compounds

It is well known that the TRPA subfamily channels in insects and vertebrates are activated by a variety of pungent natural compounds and environmental irritants,

including electrophiles (28, 31–34). We therefore attempted to identify chemical compounds that either activate or inhibit BmTRPA1. Candidate activators were screened using Ca^{2+}-imaging experiments; we found that formalin, H_2O_2, cinnamaldehyde (CA), and camphor obviously increased intracellular Ca^{2+} levels of BmTRPA1-expressing cells. The effects of these compounds on BmTRPA1 were further tested using a patch-clamp method (Supplementary Fig. S5). Currents developed slowly after addition of formalin, H_2O_2, CA, and camphor, followed by slow inactivation after washout in BmTRPA1-expressing HEK293 cells. The dose-dependent activation was observed in formalin (0.0003~1%), H_2O_2 (0.05~500 mM), and CA (0.1~3 mM), but not in mock-transfected HEK293 cells (Supplementary Fig. S6). The current-voltage relationship during heat activation showed outward rectification with the reversal potential close to zero, which is strikingly similar to TRPA1 properties in other species. Currents evoked by formalin, H_2O_2, CA, and camphor were BmTRPA1-dependent: the same cells responded to heat stimulation and the chemical-evoked currents displayed the same current-voltage relationship as that of heat currents. These results suggest that BmTRPA1 is a receptor for these chemical compounds.

Treatment with BmTRPA1 chemical activators affects diapause induction, pupal body weight, and weight of cocoon shells

We tested whether the BmTRPA1 chemical activators artificially induced progeny diapause (Fig. 5a). Throughout embryogenesis, either formalin, H_2O_2, or CA was floated as a volatile substance around 15DD eggs. Although diapause eggs were never obtained from DW-treated moths, diapause eggs were oviposited by moths that

were treated with formalin, H_2O_2, or CA at the embryo stages in a dose-dependent manner (Fig. 5a). Larvae that initiated spinning late (>50% of all larvae) oviposited relatively high proportions of diapause eggs. Since it is known that 25DD pupae have extended developmental periods and heavier bodies and cocoon shells (10), we tested whether pupal and cocoon-shell weights were affected in formalin-treated pupae. Both male and female formalin-treated pupae had bodies (Fig. 5b) and cocoon shells (Fig. 5c) that were heavier than those of 15DD control pupae, and that were similar in weight to those of 25DD pupae. Next, we examined the effects of *BmTrpA1* RNAi on formalin treatment. When formalin treatment was performed throughout embryogenesis after injection of PBS or dsRNA of *BmTrpA1*, most eggs never hatched, and those that did died during larval stages. Therefore, limited formalin treatment was performed, from st. 23 until hatching. If BmTRPA1 and its chemical activators act during the sensitive period (st. 20–23), it is expected that even limited formalin treatment in the sensitive period would cause partial induction of diapause eggs in batches and would increase pupal and cocoon shell weights, as those effects were knocked down by *BmTrpA1* RNAi. Although we were able to obtain only a few pupae in this condition, the bodies and cocoon shells (Supplementary Fig. S7a and b) of female and male pupae injected with dsRNA of *BmTrpA1* tended to be lighter, in spite of formalin treatment, than those of formalin-treated control pupae, and were similar in weight to those of pupae treated with DW and injected with either PBS or dsRNA of *BmTrpA1*. Thus, *BmTrpA1* RNAi suppressed the increase in weight of the pupal body and cocoon shell obtained by formalin treatment. However, all eggs became non-diapause eggs in this condition and we could not judge the effect of RNAi on diapause induction. Collectively, BmTRPA1 chemical activators artificially induce progeny diapause and increase pupal body and

cocoon shell weights at non-diapause-inducing temperature. To confirm whether the chemical activators of BmTRPA1 efficiently activate the channel regardless of thermal conditions, we tested the chemical activation under cool conditions (<21°C; Fig. 5d–f). In thermal gradients colder than 20°C, currents developed slowly after addition of formalin, H_2O_2 (Fig. 5e and f), and CA. When chemicals were not added, BmTRPA1 was not activated at <20°C, as described above (Fig. 5d). Therefore, BmTRPA1 is responsive to formalin, H_2O_2, and CA even at temperatures <21°C.

Discussion

In general, the extent of the thermo- or photoperiod during which insects are sensitive to diapause-inducing stimuli varies considerably among species, ranging from a few days to almost an entire year, but is more restricted within species (6). In *B. mori*, temperature during the thermosensitive period must remain continuously above the threshold for long periods during embryogenesis to induce diapause. This thermosensitive property differs from processes used to detect and respond quickly to extreme variability in temperature, such as thermal nociception and thermotaxis, which provide immediate survival advantages. This suggests that the thermosensitive properties and activation process of BmTRPA1 differ from those of other known TRPA1 channels, such that BmTRPA1 may require constant or intermittent activation during the sensitive period to induce diapause. High temperature during the sensitive period is an essential and sufficient condition for induction of progeny diapause in 25DD embryos. Embryonic BmTRPA1 could be thermally activated at >21°C during embryogenesis, and an unknown signaling pathway linked to the release of DH may then be activated. Therefore, BmTRPA1 is a thermosensitive TRP channel that acts as a molecular switch for diapause induction and for the development of an alternative phenotype in an animal with seasonal polyphenism. However, the effect of *BmTrpA1* RNAi on both diapause induction and treatment with BmTRPA1 chemical activator was weak and variable. Therefore, BmTRPA1 may play a partial role in the signaling, and other unidentified factors (e.g., cold-sensitive thermosensors activated at ≤ 15°C) may also be involved in diapause induction.

It has been speculated that in cases of seasonal polyphenism, environmental information is stored and later transduced to neuroendocrine signals via neural

remodeling in order to induce the alternative phenotype. However, identification of the molecular signals involved has not yet been accomplished (6). Consistent with this notion, we revealed that *BmTrpA1* knockdown affects DH accumulation in SLb neurosecretory cells in the SG during pupal-adult development. The reception of thermal information in 25DD probably activates the unknown signal transduction pathway, thereby causing neural and brain remodeling. This coordinates the operation of neural circuits, including regulation of dendritic growth, neural activity, and neuromodulator release. The release of DH is a critical step for the induction of diapause eggs, which was suppressed by *BmTrpA1* knockdown. We have therefore identified the first molecular pathway participating in a long-term predictive adaptive response in seasonal developmental plasticity processes. In addition, *BmTrpA1* knockdown affects the duration of growth in the larval period. Because insulin and insulin-like peptides (ILPs) can stimulate the production of ecdysteroids and juvenile hormone in *Drosophila,* and as this signaling system ultimately regulates growth rate and is essentially identical in insects and vertebrates (35), BmTRPA1 signaling may help to modify the action of factors such as ILPs and/or their signaling pathways, which would affect growth rate in addition to DH release. Furthermore, high expression of the *BmTrpA1* mRNA was observed in various tissues during larval-pupal development and after the sensitive period during embryogenesis (Fig. 3a), suggesting that BmTRPA1 may participate in other unknown physiological processes.

We observed that BmTRPA1 is ubiquitously expressed in non-neural epidermal cells in various embryonic tissues. This is different from the expression of other known insect thermosensitive TRPA subfamily members, which are primarily localized in peripheral sensory neurons and the central nervous system (CNS) in all life

stages. These TRPAs are part of the system of transduction, integration, and rapid response to heat and chemical stimuli (23, 27, 28, 36–38). Recent in vitro and in vivo studies have provided evidence that both TRPA1 and TRPV3 channels are expressed in non-neural cells, including skin epithelial cells in vertebrates (39-41). Furthermore, it has been proposed that TRPV3 in the skin may release diffusible molecules, such as adenosine triphosphate, which would then mediate thermotransduction in skin (41). This situation may apply to BmTRPA1. We speculate that the epidermal cells receive environmental temperature cues using the broadest and largest available interface with the external environment when these signals are not necessary for rapid and immediate responses through neuronal integration and behavior. Our findings suggest that non-neural insect embryonic cells may participate in thermosensitive events through TRP channel activation. Further study of the molecular mechanism is required to determine how thermosensation in non-neural cells causes DH release, which functions via transduction mechanisms, neural plasticity, and storage mechanisms.

Because 25DD pupae have extended developmental periods, heavier bodies and cocoon shells, and later lay a larger quantity of eggs than 15DD pupae, research into embryonic diapause as it relates to the prosperity of the sericulture industry in Japan began in the early 20th century (10). We showed that chemical treatment can result in moths with diapause-type characteristics, such as oviposition of diapause eggs and heavy pupal and cocoon-shell weight. These results indicate that BmTRPA1 may be a good target for controlling seasonal polyphenism in silk moths to maximize the efficiency of silk production. It has been suggested that insect TRPAs represent potential targets for disrupting thermal preferences and other thermosensory behaviors in agricultural pests and disease vectors (34). Our findings suggest that chemical ligands

of insect TRPA1 and TRPA subfamily members may be used as a new class of compounds for pest control through perturbation of seasonal polyphenism.

Materials and Methods

Silkworms

Bivoltine (Kosetsu) and polyvoltine (N4) strains of *B. mori* were used in these experiments. Insects were reared as described previously (16). During the larval stages, animals were reared at 25–27°C under a 12-h light/dark cycle and relative humidity of 50–60%. Kosetsu eggs were incubated under two different conditions throughout embryogenesis: at 25°C (25DD) or at 15°C (15DD) under continuous darkness, to obtain diapause or non-diapause eggs, respectively. The embryos were staged using a light microscope and stages were numbered from 1 to 30 based on morphological markers, as described previously (9, 42). The eclosed moths were allowed to oviposit overnight and these eggs were incubated at 26–27°C. Diapause eggs were identified as those that were colored dark brown on day 3 and remained unhatched at 2 wk after oviposition, at which time all non-diapause eggs had hatched. Both diapause and non-diapause egg-inducing activity were estimated by counting the numbers of eggs in diapause and those not in diapause after the non-diapause eggs hatched. The results are expressed as percentages of diapause or non-diapause eggs in each egg batch (43).

cDNA cloning

We found highly homologous sequences from *Bombyx* whole-genome shotgun and KAIKO cDNA databases by searching the tblastx program of KAIKOBLAST (http://kaikoblast.dna.affrc.go.jp/) against *Drosophila melanogaster TrpA1* (AY302598), *Painless* (AY268106), *Pyrexia* (NM_138171), and *Wtrw* (NM_169200). Each partial cDNA sequence was determined by RT-PCR using the first-strand DNA derived from eggs at st. 22 and pupal brain-SG complexes as templates using the specific primer sets

shown in Table S1. The full-length cDNA sequences were determined using a SMART RACE cDNA amplification kit (Clontech). Finally, the open reading frame (ORF) sequences of *BmTrpA1* (AB243445, AB703646), *BmPainless* (AB264789), *BmPyrexia* (AB437368), *BmWtrw* (AB437369), and *BmTrpA4* (AB703647) were amplified by RT-PCR.

Embryonic RNA interference (RNAi)

RNAi procedures were adapted from Masumoto et al. (44) with some modifications. The synthesis of double-stranded RNA (dsRNA) was performed by a T7 RiboMAX Express RNAi System (Promega) using the primers shown in Table S1. The concentration of dsRNAs was adjusted to 3 μg/μl. For injection into eggs, non-diapause eggs of the bivoltine strain (Kosetsu) were collected within 2 h of oviposition during the syncytial blastoderm stage. Then, dsRNA was injected into eggs using a glass needle (uMPm-02; Daiwa Union) attached to a manipulator (kaikopuchu-STDU1; Daiwa Union) and FemtoJet (Eppendorf). Eggs injected with dsRNA were incubated at 25°C in moist conditions until hatching.

RT-PCR analysis

Eggs were collected from 0.2 d after oviposition until day 9.0 (25DD) or day 34 (15DD) of eclosion at each developmental stage and stored at –80°C until use. Poly $(A)^+$ RNAs were prepared according to Shiomi et al. (45) using Dynabeads Oligo $(dT)_{25}$ (Dynal Biotech LLC). First-strand DNA was synthesized using a SMART RACE amplification kit (Clontech); mRNA PCR amplification was carried out for *BmTrpA1* and *ActA3*. We amplified the +1053 to +1930 region of a *BmTrpA1* cDNA (AB703646),

and region +70 to +498 of an *ActA3* cDNA (AB701689) using the primers shown in Table S1. The PCR products were subjected to electrophoresis and then visualized with ethidium bromide staining.

Histochemical analysis

Standard protocols were used for immunohistochemistry as previously described (16, 29). For anti-BmTRPA1 immunohistochemistry, we used an anti-BmTRPA1 mouse antibody prepared from mice immunized with BSA-conjugated 14 amino acid coding sequences from R1134 to A1147 of the BmTRPA1. The anti-BmTRPA1 IgG was purified by NAb^{TM}Protein A/G Spin Columns (Thermo). *BmTrpA1*-transfected HEK293 cells were processed for immunostaining as described in Matsuura et al. (29). Anti-BmTRPA1 antibody was used at 500-fold dilution. The Alexa Fluor® 488-labeled anti-mouse IgG (Hypromatrix) was used for the second antibody. For immunostaining of embryos, both the anti-BmTRPA1 (100-fold dilution) and Cy3-labeled anti-mouse F(ab′)$_2$ antibodies (Jackson ImmunoResearch) were incubated with embryos overnight. The fluorescence signals were detected using an Olympus FV1000-D confocal microscope (Olympus). Images were adjusted and assembled using Adobe Photoshop CS3 (Adobe Inc.). The immunoreaction procedure for the anti-DH antibody was adapted from Hagino et al. (16). Images were acquired by an Olympus FV1000-D confocal microscope and analyzed with NIH Image 1.62 (http://rsb.info.nih.gov/nih-image/) as previously described (16). To determine the relative fluorescence intensity of the SLb cells, we compared the intensity of the mean pixel fluorescence for individual somata. Images to be compared were processed identically and image capture was set to avoid fluorescence saturation. Analysis was

performed as described previously (16). Data were presented as the percentage intensity relative to the mean intensity of the control. *Bombyx* CNS terminology followed Sato et al. (46). For SEM observation, dissected embryos were fixed and dehydrated as described in Hagino et al. (16). The embryos were dried in liquid nitrogen and observed using a JSM-6010LA scanning electron microscope (JEOL Ltd.).

Western blot analysis

Embryos were dissected from eggs 4.0, 5.5, and 9.0 d after oviposition and homogenized in 1× SDS sample buffer. Eggs at 1.0 d after oviposition were directly homogenized in 1× SDS sample buffer. After separation by 7.7% SDS-PAGE, proteins were transferred to an Immobilon-P PVDF membrane (Millipore), which was then incubated with anti-BmTRPA1 antibody at 1000-fold dilution at 4°C overnight. The signals were detected using horseradish peroxidase-linked goat anti-mouse IgG (Invitrogen) and ECL-Plus Western blotting detection reagents (GE Healthcare).

Ca^{2+} imaging and patch-clamp analyses

For construction of the BmTRPA1-expressing vector for mammalian cells (human embryonic kidney 293T cells; HEK 293), the ORF sequence of *BmTrpA1* was amplified by PCR using the primers shown in Table S1. The ORF sequence was then inserted into a pcDNA3 vector (Invitrogen). This recombinant vector was co-transfected with DsRed or pGreen Lantern-1 marker into HEK293 cells using Lipofectamine (Invitrogen) and the cells were cultured for 20–40 h at 33°C. These transient-transfected cells were used for Ca^{2+} imaging and patch-clamp analyses. Procedures adapted from Kohno et al. (28) were used for Ca^{2+} imaging and patch-clamp recording.

Egg treatment with chemical ligands of BmTRPA1

Egg treatment with chemical ligands of BmTRPA1 was carried out in plastic petri dishes (60-mm diameter). Each egg batch (200–300 eggs) oviposited on drafting paper by newly eclosed females was sterilized with 3% formalin for 5 min, dried, and mounted onto the underside of a Petri dish lid using double-stick tape. Formalin, H_2O_2, and CA were serially diluted and added to the bottom of the Petri dishes, which were then sealed with Parafilm and incubated at 15°C in continuous darkness. Embryonic development was checked by observing eggs incubated with continuous illumination. The day before hatching, each egg batch was transferred to a 12-h light/dark cycle at 25°C until hatching.

Statistical analysis

Data were compared using Student's *t*-tests. Multiple comparisons were performed using Tukey's tests. The significance of differences presented in Figures 1b, 5a, and S2a was evaluated using the Steel-Dwass test. Statistical analyses were performed in Excel 2011 (Microsoft) with the software add-in Toukei-Kaiseki Ver. 2.0 (Esumi).

Acknowledgements

We thank Y. Kubota, D. Kumamoto, and H. Miyazawa for silkworm rearing. We also thank K. Kakegawa for SEM observations, and Dr. Y. Matsumura for useful discussion on statistical analysis. This research was funded by Grants-in-Aid from the Ministry of Education, Science, Sports and Culture of Japan, and supported partly by NAITO Foundation. We are also indebted to the Division of Gene Research, Research Center for Human and Environmental Sciences, and VBL at Shinshu University for providing facilities for these studies.

References

1. West-Eberhard MJ (2003) *Developmental Plasticity and Evolution* (Oxford Univ Pr (Sd)).
2. Gilbert SF & Epel D (2009) How agents in the environment effect molecular changes in development. *Ecological Developmental Biology: Integrating Epigenetics, Medicine, and Evolution*, eds Gilbert SF & Epel D (Sinauer Associates Inc.), pp 38-78.
3. Mousseau TA & Fox CW (1998) *Maternal effects as adaptations* (Oxford University Press).
4. Gluckman PD, Hanson MA, & Spencer HG (2005) Predictive adaptive responses and human evolution. *Trends Ecol Evol* 20(10):527-533.
5. Kostal V (2006) Eco-physiological phases of insect diapause. *J Insect Physiol* 52(2):113-127.
6. Tauber MJ, Tauber CA, & Masaki S (1986) *Seasonal Adaptations of Insects* (Oxford University press).
7. Nijhout HF (2003) Development and evolution of adaptive polyphenisms. *Evol Dev* 5(1):9-18.
8. Watanabe K (1924) Studies on the voltinism of the silkworm, *Bombyx mori*. *Bull Sericult Exp Sta (Tokyo)* 6:411-455.
9. Morita A, Niimi T, & Yamashita O (2003) Physiological differentiation of DH-PBAN-producing neurosecretory cells in the silkworm embryo. *J Insect Physiol* 49(12):1093-1102.
10. Yamashita O & Yaginuma T (1991) Silkworm eggs at low temperatures: Implication for sericulture. *Insects at Low Temperature*, eds Lee JRE & Denlinger DL (Chapman and Hall, New York), pp 424-445.
11. Xu WH, Sato Y, Ikeda M, & Yamashita O (1995) Stage-dependent and temperature-controlled expression of the gene encoding the precursor protein of diapause hormone and pheromone biosynthesis activating neuropeptide in the silkworm, *Bombyx mori*. *J Biol Chem* 270(8):3804-3808.
12. Yamashita O (1996) Diapause hormone of the silkworm, *Bombyx mori*: structure, gene expression and function. *J Insect Physiol* 42:669-679.
13. Homma T, et al. (2006) G protein-coupled receptor for diapause hormone, an inducer of *Bombyx* embryonic diapause. *Biochem Biophys Res Commun* 344(1):386-393.
14. Sato Y, et al. (1993) Precursor polyprotein for multiple neuropeptides secreted from the suboesophageal ganglion of the silkworm Bombyx mori: characterization of the cDNA encoding the diapause hormone precursor and identification of additional peptides. *Proc Natl Acad Sci USA* 90(8):3251-3255.
15. Sato Y, Ikeda M, & Yamashita O (1994) Neurosecretory cells expressing the gene for common precursor for diapause hormone and pheromone biosynthesis-activating neuropeptide in the suboesophageal ganglion of the silkworm, *Bombyx mori*. *Gen Comp Endocrinol* 96(1):27-36.
16. Hagino A, Kitagawa N, Imai K, Yamashita O, & Shiomi K (2010) Immunoreactive intensity of FXPRL amide neuropeptides in response to environmental conditions in the silkworm, *Bombyx mori*. *Cell Tissue Res* 342(3):459-469.

17. Kitagawa N, et al. (2005) Establishment of a sandwich ELISA system to detect diapause hormone, and developmental profile of hormone levels in egg and subesophageal ganglion of the silkworm, *Bombyx mori*. *Zoolog Sci* 22(2):213-221.
18. Clapham DE (2003) TRP channels as cellular sensors. *Nature* 426(6966):517-524.
19. Dhaka A, Viswanath V, & Patapoutian A (2006) Trp ion channels and temperature sensation. *Annu Rev Neurosci* 29:135-161.
20. Fowler MA & Montell C (2013) Drosophila TRP channels and animal behavior. *Life sciences* 92(8-9):394-403.
21. Wetsel WC (2011) Sensing hot and cold with TRP channels. *International journal of hyperthermia: the official journal of European Society for Hyperthermic Oncology, North American Hyperthermia Group* 27(4):388-398.
22. Viswanath V, *et al.* (2003) Opposite thermosensor in fruitfly and mouse. *Nature* 423(6942):822-823.
23. Rosenzweig M, *et al.* (2005) The *Drosophila* ortholog of vertebrate TRPA1 regulates thermotaxis. *Genes Dev* 19(4):419-424.
24. Hamada FN, *et al.* (2008) An internal thermal sensor controlling temperature preference in Drosophila. *Nature* 454(7201):217-220.
25. Rosenzweig M, Kang K, & Garrity PA (2008) Distinct TRP channels are required for warm and cool avoidance in *Drosophila melanogaster*. *Proc Natl Acad Sci USA* 105(38):14668-14673.
26. Gallio M, Ofstad TA, Macpherson LJ, Wang JW, & Zuker CS (2011) The coding of temperature in the *Drosophila* brain. *Cell* 144(4):614-624.
27. Wang G, *et al.* (2009) *Anopheles gambiae* TRPA1 is a heat-activated channel expressed in thermosensitive sensilla of female antennae. *Eur J Neurosci* 30(6):967-974.
28. Kohno K, Sokabe T, Tominaga M, & Kadowaki T (2010) Honey bee thermal/chemical sensor, AmHsTRPA, reveals neofunctionalization and loss of transient receptor potential channel genes. *J Neurosci* 30(37):12219-12229.
29. Matsuura H, Sokabe T, Kohno K, Tominaga M, & Kadowaki T (2009) Evolutionary conservation and changes in insect TRP channels. *BMC Evol Biol* 9:228.
30. Ramsey IS, Delling M, & Clapham DE (2006) An introduction to TRP channels. *Annu Rev Physiol* 68:619-647.
31. Hinman A, Chuang HH, Bautista DM, & Julius D (2006) TRP channel activation by reversible covalent modification. *Proc Natl Acad Sci USA* 103(51):19564-19568.
32. Macpherson LJ, *et al.* (2007) Noxious compounds activate TRPA1 ion channels through covalent modification of cysteines. *Nature* 445(7127):541-545.
33. Sokabe T, Tsujiuchi S, Kadowaki T, & Tominaga M (2008) *Drosophila* painless is a Ca^{2+}-requiring channel activated by noxious heat. *J Neurosci* 28(40):9929-9938.
34. Kang K, et al. (2010) Analysis of *Drosophila* TRPA1 reveals an ancient origin for human chemical nociception. *Nature* 464(7288):597-600.
35. Shingleton AW (2011) Evolution and the regulation of growth and body size. *Mechanisms of Life History Evolution. The Genetics and Physiology of Life*

History Traits and Trade-Offs, eds Flatt T & Heyland A (Oxford University Press), pp 43-55.
36. Tracey WD, Jr., Wilson RI, Laurent G, & Benzer S (2003) *Painless*, a *Drosophila* gene essential for nociception. *Cell* 113(2):261-273.
37. Lee Y*, et al.* (2005) Pyrexia is a new thermal transient receptor potential channel endowing tolerance to high temperatures in *Drosophila melanogaster*. *Nat Genet* 37(3):305-310.
38. Al-Anzi B, Tracey WD, Jr., & Benzer S (2006) Response of *Drosophila* to wasabi is mediated by painless, the fly homolog of mammalian TRPA1/ANKTM1. *Curr Biol* 16(10):1034-1040.
39. Cao DS*,* et al*.* (2012) Expression of transient receptor potential ankyrin 1 (TRPA1) and its role in insulin release from rat pancreatic beta cells. *PLoS One* 7(5):e38005.
40. Nozawa K*, et al.* (2009) TRPA1 regulates gastrointestinal motility through serotonin release from enterochromaffin cells. *Proc Natl Acad Sci USA* 106(9):3408-3413.
41. Mandadi S*,* et al*.* (2009) TRPV3 in keratinocytes transmits temperature information to sensory neurons via ATP. *Pflugers Arch* 458(6):1093-1102.
42. Takami T & Kitazawa T (1960) External observation of embryonic development in the silkworm. *Bull Sericult Exp Sta (Tokyo)* 75:1-31.
43. Yamashita O & Hasegawa K (1985) Embryonic diapause. *Comprehensive Insect Physiology, Biochemistry and Pharmacology*, eds Kerkut GA & Gilbert LI (Pergamon Press, Oxford), Vol 1, pp 407-434.
44. Masumoto M, Yaginuma T, & Niimi T (2009) Functional analysis of Ultrabithorax in the silkworm, *Bombyx mori*, using RNAi. *Dev Genes Evol* 219(9-10):437-444.
45. Shiomi K*,* et al*.* (2005) Myocyte enhancer factor 2 (MEF2) is a key modulator of the expression of the prothoracicotropic hormone gene in the silkworm, *Bombyx mori*. *Febs J* 272(15):3853-3862.
46. Sato Y, Shiomi K, Saito H, Imai K, & Yamashita O (1998) Phe-X-Pro-Arg-Leu-NH(2) peptide producing cells in the central nervous system of the silkworm, *Bombyx mori*. *J Insect Physiol* 44(3-4):333-342.

Figure legends

Figure 1. Embryonic RNAi knockdown of *BmTrpA1* induces non-diapause eggs in progeny. (**a**) Schematic representation of embryonic diapause in the progeny of the silkworm, *Bombyx mori*. Progeny diapause is determined by environmental temperature during the sensitive period (stages 20–23) of the mother's embryonic development. When eggs are incubated at 25°C, the resultant female moths (25DD) lay pigmented diapause eggs. In contrast, incubation at 15°C causes the resultant moths (15DD) to lay non-diapause eggs. Non-diapause eggs complete their embryogenesis approximately 9 d after oviposition at 25°C. In contrast, diapause eggs remain in the diapause stage (stage 8). In 25DD pupae, diapause hormone released into the hemolymph acts on a G-protein coupled receptor, DH receptor. (**b**) Effect of dsRNA injection on diapause-egg-inducing activity. Double-stranded RNA of *TrpA* subfamily genes (*trpA1*, *painless*, *pyrexia*, *wtrw*, and *trpA4*) and *EGFP* were injected into newly laid, non-diapause eggs. Non-diapause egg-inducing activity is represented as the percentage of oviposited eggs in each batch that were non-diapause eggs; *trpA1* (D19) and *trpA1* (D20–23) indicate *BmTrpA1* RNAi-injected larvae that initiated spinning at 19 d and at 20–23 d respectively. Data represent means ± SD. **, $P < 0.01$ vs. PBS (25DD). (**c**) Effect of *BmTrpA1* dsRNA injection on initiation of spinning. Larval growth rates are represented as days between hatching and initiation of spinning in final- (fifth-) instar larvae. The larvae were checked twice daily at 8:00 AM and 5:00 PM. In **b** and **c,** N (egg batch) = 84 (PBS, 25DD); N = 31 (*EGFP,* 25DD); N = 84 (*trpA1,* 25DD); N = 81 (others, 25DD); N = 10 (PBS and *trpA1*, 15DD); and N = 81 (non-injected control, 15DD) in **c**.

Figure 2. Developmental expression profiles of *BmTrpA1*. (**a**) RT-PCR analysis was

performed on 25DD and 15DD during embryonic development. The mRNA levels of *BmTrpA1* in 25DD and 15DD (TRPA1, lanes 1–19 and 39–57 respectively) and *ActinA3* in 25DD and 15DD (ActA3, lanes 20–38 and lanes 58–76 respectively) were examined. The shaded area indicates the sensitive periods (stage; st.). (**b–d**) SEM observation of the lateroventral view at stage 20 (**b**), and lateral view at stages 21 (**c**) and 23 (**d**) of embryonic development. The head in (**c)** is indicated by red pseudo-color. Each box indicates the body part examined using immunohistochemistry in (**f)**, (**g)**, (**i–k)**. The arrow indicates yolk granules taken from around the dorsal closure. Scale bar = 100 μm. (**e**) Distribution of *BmTrpA1* mRNA in embryos. Whole embryos (E) and yolk (Y) were separated from stage-21 eggs of 25DD and the embryos were dissected to separate the head (H, indicated in [**c**]) and thorax and abdomen complex (T+A, indicated in [**c**]). Dissected tissues were subjected to RT-PCR analysis of *BmTrpA1* (TRPA1, lanes 1–4) and *ActA3* (ActA3, lanes 5–8) mRNAs. (**f–k**) Whole-mount immunohistochemistry was performed using anti-BmTRPA1 antibody at embryo stages 20–23. Immunoreactive signals (red) were detected in the caudal region of stage-20 embryos (**f**), anal prolegs of stage-23 embryos (**i**), prolegs of stage-21 embryos (**g** and **h**), prolegs of stage-23 embryos (**j**), and the hump with bristle (socket cell) in stage-23 embryos (**k**). Arrowheads indicate the immunoreactive signals in each specimen. Asterisks indicate each proleg. The prolegs of stage-21 embryos were stained with DAPI (blue) (**h**). Magnified images of the tips of prolegs are shown in insets (**i–j**). Scale bar = 25 μm (**f–J**) and 10 μm (**k**).

Figure 3. *BmTrpA1* knockdown affects immunoreactive intensity of SLb somata in DHPCs. (**a–d**) Representative images of immunohistochemistry of pupal

subesophageal ganglion (SG) using anti-diapause hormone (anti-DH) antibody. Images are of 15DD (**a**), and 25DD (**b**). Also shown are results from pupae injected with *BmTrpA1* dsRNA (**c**), and *EGFP* dsRNA (**d**). The dsRNA was injected into newly laid eggs, and the pupal SG was dissected out 4 d after pupation. The arrow indicates the SLb somata. (**e**) The relative fluorescence intensity in the SLb somata is reported as a percentage of that for 15DD. Each bar represents the mean value of 30 samples ± SD. ***, $P < 0.001$ vs. 25DD.

Figure 4. BmTRPA1 is a thermosensitive TRP channel. (**a**) BmTRPA1-expressing cells were identified using coexpressed DsRed protein (left panel). Representative results are shown for Fura-2 Ca^{2+} imaging at 25.1°C, 15.4°C, and 43.7°C. The pseudocolor indicates intensity of the 340/380-nm fluorescence ratio. (**b**) Temporal changes in the Fura-2 ratio in BmTRPA1-expressing cells (top) and temperature (bottom) in the presence of 2 mM extracellular Ca^{2+}. The average trace (red line) ± SD is shown at the top. Ionomycin was added at 240 s (Iono, gray bar), N = 85. (**c**) Temporal changes in the current (top trace) in a BmTRPA1-expressing cell and temperature (bottom trace) during temperature-fluctuation voltage-clamp whole-cell in patch-clamp analysis. Holding potential was –60 mV throughout the experiment. (**d**) Representative temperature-response profile for heat-induced BmTRPA1 current, as observed in (**c**). (**e**) An Arrhenius plot for the heat-induced BmTRPA1 current shows a clear flex point in temperature dependency (data in [**d**] were converted). The temperature threshold for BmTRPA1 activation was defined as the point at which the two linear-fitted lines crossed (a flex point). The Q_{10} value was calculated for each line.

Figure 5. Chemical compounds activate BmTRPA1 independently of heat, induce diapause, and increase body and cocoon-shell weight. (**a**) Effect of treatment with chemical compounds on diapause-egg-inducing activity. Eggs were incubated at 15DD with formalin, H_2O_2, and CA, and the percentage of diapause eggs produced by their progeny was calculated. The moths were divided into two groups: larvae that initiated spinning earlier (<50% of total larvae; early), and larvae that initiated spinning later (>50% of total larvae; late). **(b**–**c**) Effects on pupal and cocoon-shell weights. Eggs were incubated at 25°C or 15°C in the dark with or without 0.3% formalin. Pupae (**b**) and cocoon-shell (**c**) weights after 3 d of pupation are shown. In **a**–**c**, 15DD (N = 54), 25DD (N = 141, as in Fig. 1), formalin (0.003%; N = 23, 0.03%; N = 46, 0.3%, N = 87), H_2O_2 (0.5 mM; N = 64, 5 mM; N = 68, 50 mM; N = 72), CA (0.01 mM; N = 52, 0.1 mM; N = 53, 1 mM; N = 44). Data represent means ± SD. ***, $P < 0.001$; **, $P < 0.01$; *, $P < 0.05$. In (**a)**, lower-case letters indicate statistically significant differences in DW-treated vs. chemical-compound-treated animals (**a**), and early vs. late animals (**b**). (**d**–**f**) Temporal changes in current (top trace) in a BmTRPA1-expressing cell, and temperature (bottom trace) during temperature fluctuation without additional chemical compounds (**d**), with 0.01% formalin (**e**), and 10 mM H_2O_2 (**f**) during cooling in a whole-cell patch-clamp experiment. Membrane potential was held at –60 mV. Note that a sudden increase in current level was observed after H_2O_2 washout, probably because currents were still gradually developing at that time and were enhanced by the temperature increase.

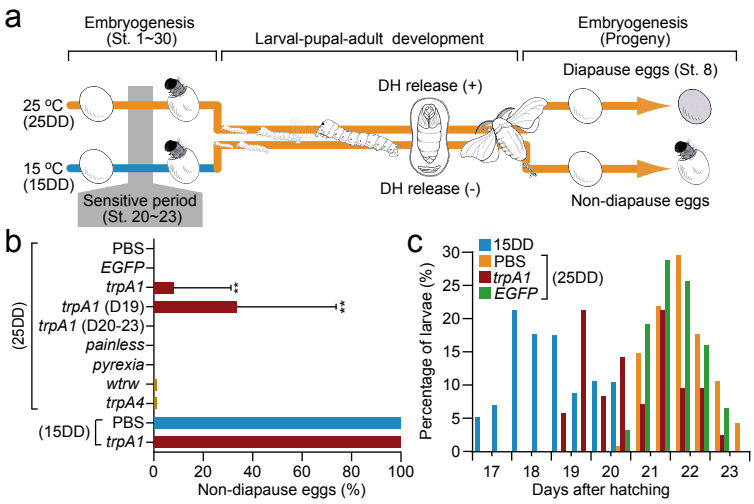

Fig. 1. (Sato & Sokabe et al.)

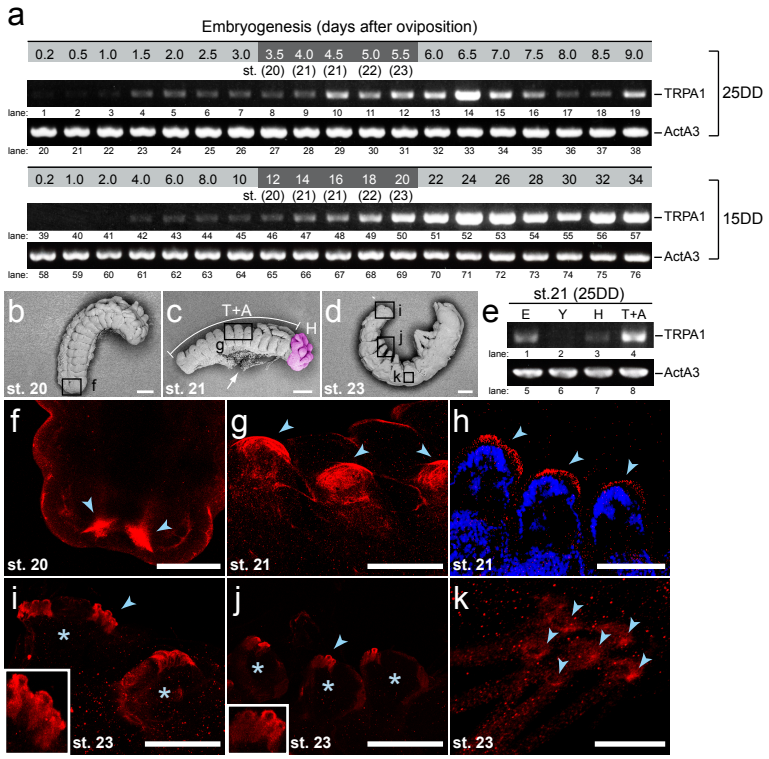

Fig. 2. (Sato & Sokabe et al.)

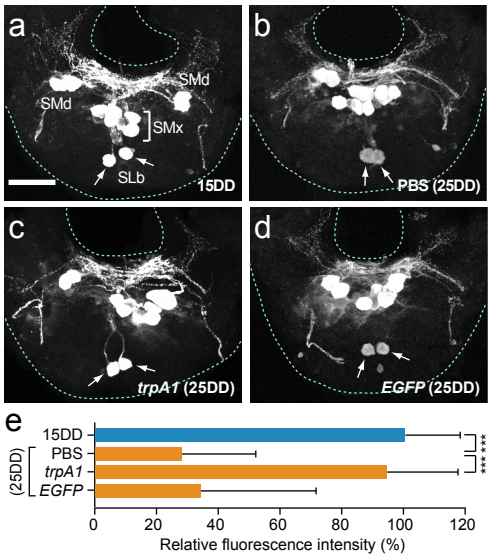

Fig. 3. (Sato & Sokabe et al.)

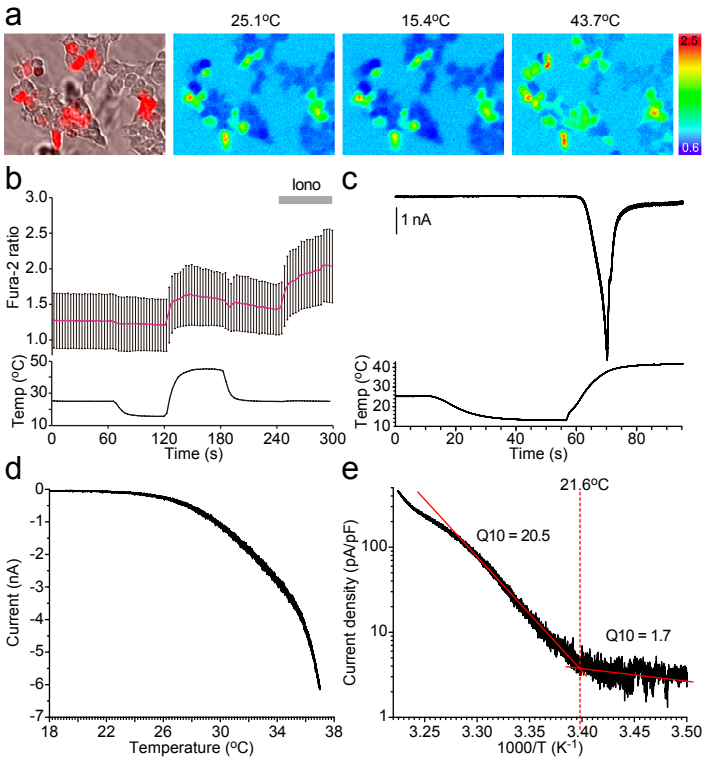

Fig. 4. (Sato & Sokabe et al.)

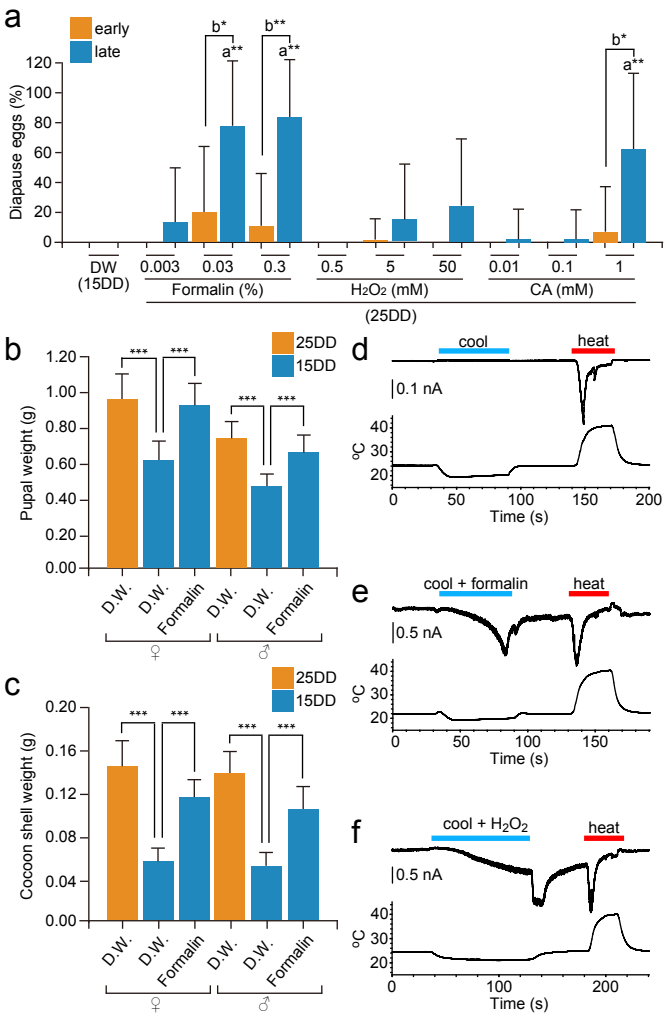

Fig. 5. (Sato & Sokabe et al.)

Suplementary Table S1. List of primers

a. For cDNA cloning		
1. *TrpA1*		Forward: 5' -AGCGGAAATGTCGATGACTTCATGCGATTG-3'
		Reverse: 5' -GTTGTGATGAATGAGAAATATCTCTATTTC-3'
2. *Painless*		Forward: 5' -GGAAATCGGTCTTATTTTTGTGACGATTTG-3'
		Reverse: 5' -CGCGCTACCGATAAGCACGCTCTCGATGTA-3'
3. *Pyrexia*		Forward: 5 '-AAACGTTTCTGTTTTTGAAATGGCGCAGAA-3'
		Reverse: 5' -CTGGATATCACTAACAGCTAAACCAACTAG-3'
4. *Wtrw*		Forward: 5' -GCACCCAATATGTACGACAGCTTCGAGGAG-3'
		Reverse: 5' -TAGGCAGTCTCTTCTCGCTTGGGTTCAACG-3
5. *TrpA4*		Forward: 5' -CGGCGGATCCGCGAGATGGGGTGGCCTTCA-3'
		Reverse: 5' -ATGCGCGGTGTACATGGACATTTAAATCTT-3'
b. For dsRNA synthesis		
1. *TrpA1*	*#1* (2020-2520)*	Forward: 5' -GAATTAATACGACTCACTATAGGGAGAGCCTTACGTTCAGA-3'
		Reverse: 5' -GAATTAATACGACTCACTATAGGGAGAGAAATCTGCATCAA-3'
	#2 (3160-3660)**	Forward: 5' -GAATTAATACGACTCACTATAGGGAGACAGCTGAAACGGCT-3'
		Reverse: 5' -GAATTAATACGACTCACTATAGGGAGAGAAATATCTCTATT-3'
2. *Painless*	*#1* (1341-1841)*	Forward: 5' -GAATTAATACGACTCACTATAGGGAGAGAACTACTTAGAAA-3'
		Reverse: 5' -GAATTAATACGACTCACTATAGGGAGATGTGATAACGTTTA-3'
	#2 (2461-2961)**	Forward: 5' -GAATTAATACGACTCACTATAGGGAGACAGATGCCGAATTA-3'
		Reverse: 5' -GAATTAATACGACTCACTATAGGGAGAATATTCTTTAGTAT-3'
3. *Pyrexia*	*#1* (1179-1680)*	Forward: 5' -GAATTAATACGACTCACTATAGGGAGATTCTGACAATTTCG-3'
		Reverse: 5' -GAATTAATACGACTCACTATAGGGAGAACTGGGCGGAGATA-3'
	#2 (2379-2880)**	Forward: 5' -GAATTAATACGACTCACTATAGGGAGAGCAGTTGCTGACTG-3'
		Reverse: 5' -GAATTAATACGACTCACTATAGGGAGAACATTTTACGGCAG-3'
4. *Wtrw*	#1 (2260-2760)*	Forward: 5' -GAATTAATACGACTCACTATAGGGAGAACCGCCGGCCTTTC-3'
		Reverse: 5' -GAATTAATACGACTCACTATAGGGAGATGACAGGCAATTAT-3'
	#2 (1159-1659)**	Forward: 5' -GAATTAATACGACTCACTATAGGGAGATTGATATATCACGG-3'
		Reverse: 5' -GAATTAATACGACTCACTATAGGGAGATTCAATTACGAATG-3'
5. *TrpA4*	#1 (2581-3081)*	Forward: 5' -GAATTAATACGACTCACTATAGGGAGAAAGGAAGACAGCAGG-3'
		Reverse: 5' -GAATTAATACGACTCACTATAGGGAGAGAAGCATGCTGGGAT-3'
	#2 (1579-2079)**	Forward: 5' -GAATTAATACGACTCACTATAGGGAGAAACTCCTAAGTCTCT-3'
		Reverse: 5' -GAATTAATACGACTCACTATAGGGAGATGGTAGAAACTCGAG-3'
6. *EGFP* *		Forward: 5' -GAATTAATACGACTCACTATAGGGAGATTCAGCCGCTACCC-3'
(pEGFP-1: 310-810)		Reverse: 5' -GAATTAATACGACTCACTATAGGGAGAGTACAGCTCGTCCA-3'
c. For RT-PCR analysis		
1. *TrpA1*		Forward: 5' -CCCTCTGGATAAGGAGCGAAGGTC-3'
		Reverse: 5' -AGGCGATGAGAGCCAAGGTCACGC-3'
2. *ActA3*		Forward: 5' -ATGTGCGACGAAGAAGTTGCCGCGTTG-3'
		Reverse: 5' -CAGCGAGAGCACGGCTTGGATGGCGAC-3'
d. For Ca2+ imaging and patch-clamp analyses		
		Forward: 5' -GGATCCGTTATGGGTTCGTTCAATCAATCG-3'
		Reverse: 5' -GCGGCCGCTCATCAGGTCGACTTGTTAAAT-3'

*) The diapause egg inducing activities by RNAi experiment using these primer sets were shown in Fig. 1.

**) The diapause egg inducing activities by RNAi experiment using these primer sets (#2) were shown in Fig. S1.

Sadow boxes show the T7 promoter sequences.

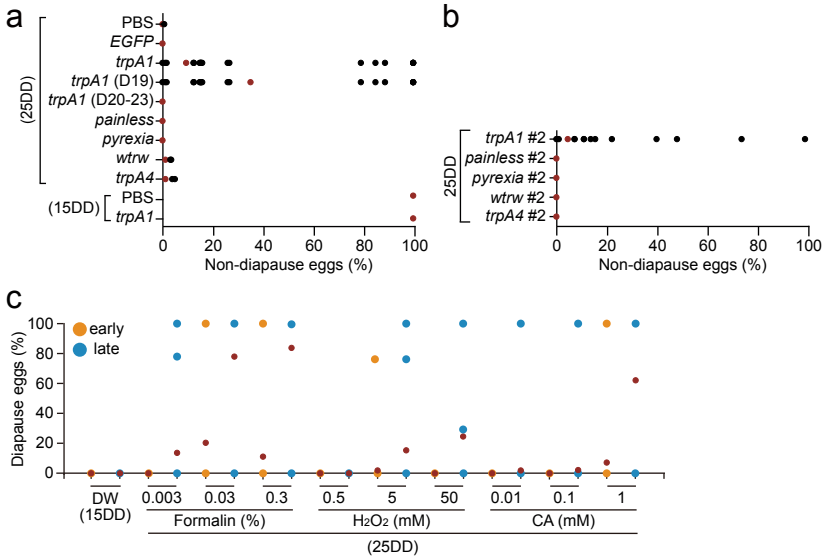

Supplementary Figure S1. The plots representation of percentages of non-diapause eggs shown in Figs. 1b (**a**) and S2a (**b**), and diapause eggs shown in Fig. 5a (**c**). In each batch, the percentages of non-diapause or diapause-egg-inducing activities were plotted. Red circles show means.

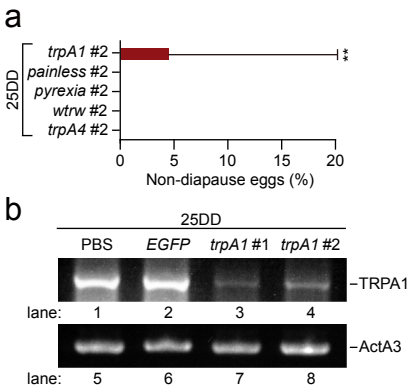

Supplementary Figure S2. (a) Diapause-egg-inducing activity of RNAi using primer set #2 in Table S1. dsRNA of each TrpA subfamily was synthesized using primer set #2 shown in Table S1. The non-diapause-egg-inducing activity of the dsRNA is presented as in Fig. 1. Data represent means ± SD. **(b) mRNA levels of BmTrpA1 after dsRNA injection.** The dsRNA (trpA1 #1, trpA1 #2, EGFP) was injected into newly laid eggs and the eggs were then subjected to Poly (A)+ RNA extraction. RT-PCR was performed as described in Fig. 2 using the primers shown in Table S1.

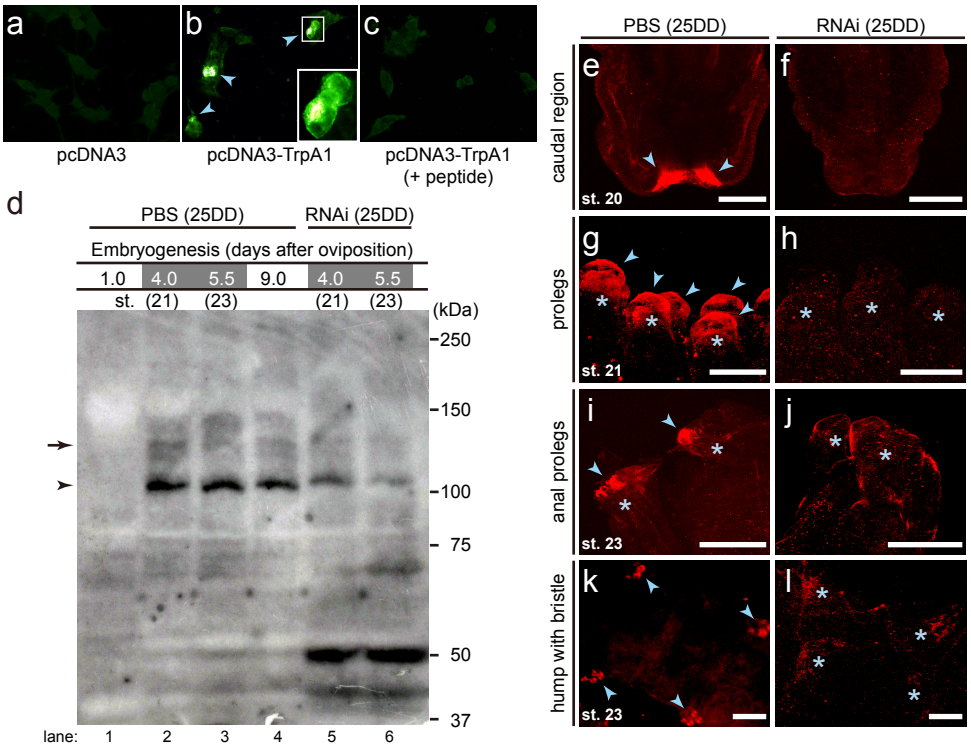

Supplementary Figure S3. (a–c) Immunostaining of BmTrpA1-transfected HEK293 cells. The immunostaining was performed in HEK293 cells transfected with vector only (**a**) and with *BmTrpA1* cDNA (**b**, **c**). In (**c**), antigenic peptide (the amino acid sequences from R1134 to A1147 of the BmTRPA1) was added before reaction of the anti-BmTRPA1 antibody. Arrowheads indicate the immunoreactive signals. Magnified images of the immunoreactive cells are shown in insets. (**d**) Western blot analysis. Extracts equivalent to those from the 4 eggs on day 1.0 after oviposition (lane 1), and the 4 embryos on days 4.0, 5.5, and 9.0 after oviposition (lanes 2–6) were applied to each lane. PBS (PBS, 25DD; lanes 1–4) or dsRNA of *BmTrpA1* (RNAi; lanes 5, 6) was injected into newly oviposited eggs and eggs were incubated at 25 ° C. The intense band detected at about 130 kDa is similar to the predicted molecular weight of BmTRPA1 (131.363 kDa) (arrow) and to protein detected at 110 kDa (arrowhead). Numbers on the right represent molecular size in kDa. (**e-l**) Immunostaining of RNAi embryos. Immunostaining was performed using anti-BmTRPA1 in embryos injected with PBS (**e, g, i, k**) and dsRNA of *BmTrpA1* (**f, h, j, l**) in newly oviposited eggs. Embryos were dissected on days 3.5 (st. 20), 4.5 (st. 21), and 5.5 (st. 23) after oviposition and subjected to immunostaining in the caudal region of stage-20 embryos (**e, f**), prolegs of stage-21 embryos (**g, h**), anal prolegs of stage-23 embryos (**i, j**), and the hump with bristle (socket cell) in stage-23 embryos (**k, l**). Arrowheads indicate the immunoreactive signals in each specimen. Asterisks indicate each proleg. Scale bar = 25 μm (**e–j**) and 10 μm (**k, l**).

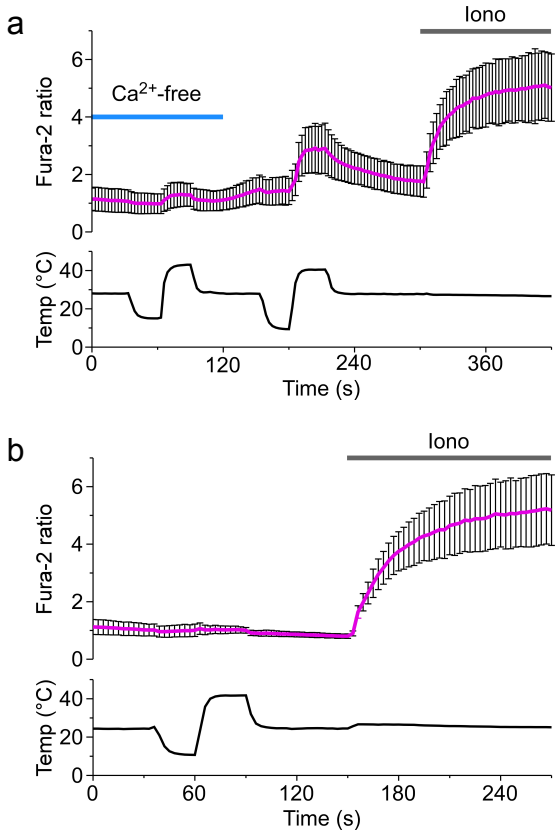

Supplementary Figure S4. (**a**) Temporal changes in the Fura-2 ratio in BmTRPA1-expressing cells (top) and temperature (bottom) in the absent of extracellular Ca^{2+} (Ca^{2+} free, blue bar) or in the presence of 2mM extracellular Ca^{2+}. The average trace (red line) ± SD is shown at the top.Ionomycin was added at 300 s (Iono, gray bar). (**b**) Mock-transfected HEK293 cells did not display heat-induced $[Ca^{2+}]i$ increase.

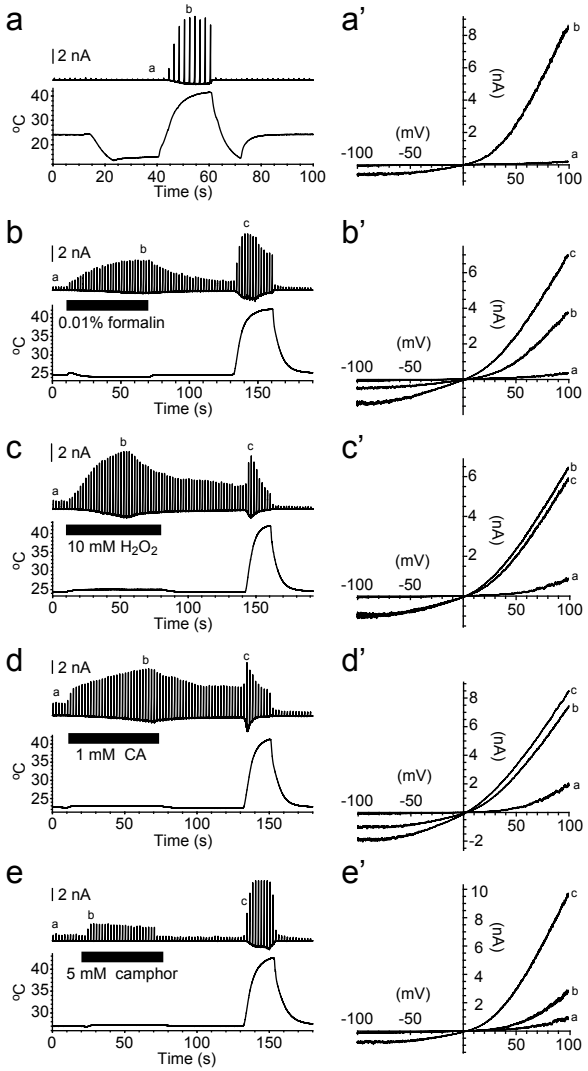

Supplementary Figure S5. BmTRPA1 is activated by chemical compounds. (**a**) Temporal changes in the current (top trace) in BmTRPA1-expressing cells and temperature (bottom trace) during treatment with heat (**a**), 0.01% formalin (**b**), 10 mM H_2O_2 (**c**), 1 mM CA (**d**), or 5 mM camphor (**e**) in whole-cell patch-clamp experiments. Membrane potential was held at –60 mV and voltage ramp pulses from –100 mV to +100 mV (500 ms) were applied every 2 s to generate an I-V curve. (**a'–e'**) Representative I-V relationships for BmTRPA1 activation with heat (**a'**), 0.01% formalin (**b'**), 10 mM H_2O_2 (**c'**), 1 mM CA (**d'**), and 5 mM camphor (**e'**). The I-V curves (**a**, **b**, and **c**) were selected from traces in **a**–**e**.

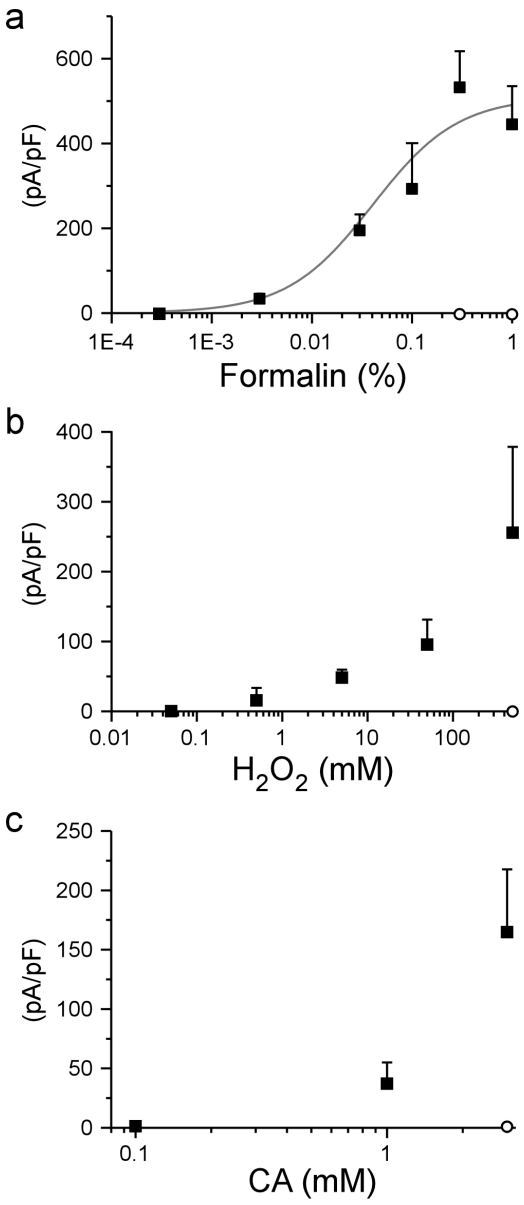

Supplementary Figure S6. Dose-dependent activation of BmTRPA1 by formalin (a), H_2O_2 (b), and CA (c). Densities (pA/pF) of the currents evoked by agonists in BmTRPA1-expressing HEK293 cells (filled squares) or mock-transfected cells (open circles) at a holding potential of –60 mV. Dose–response profile of formalin fitted with a Hill equation (EC50: 0.0406 ± 0.0142%, Vmax: 509.5 ± 69.6 pA/pF). Each data point represents the mean ± SE. (N = 4).

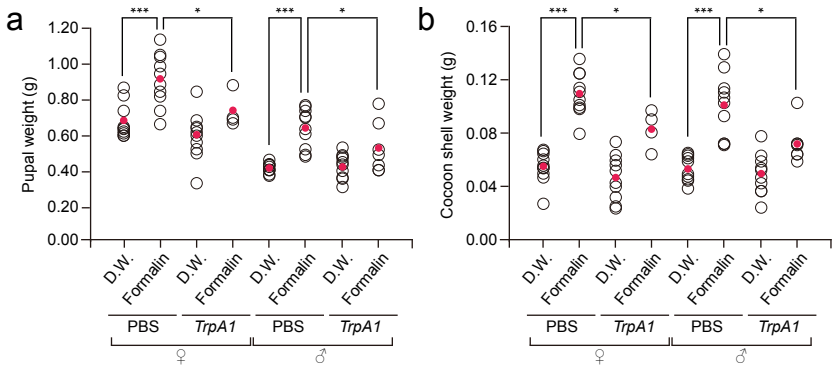

Supplementary Figure S7. Effects of BmTrpA1 RNAi on body and cocoon weights. Each dsRNA (*trpA1* #1) and PBS was injected into newly laid eggs and the eggs were then incubated at 15 ° C in the dark until stage 22. From stage 23 to hatching, the eggs were incubated with 0.3% formalin or DW. Pupae (**a**) and cocoon-shell (**b**) weights after 3 d of pupation are plotted. In both a and b, the pupae treated with formalin after injection of *BmTrpA1* dsRNA or PBS included 4 or 10 female and 7 or 10 male animals, respectively. The pupae treated with DW included 10 animals. Red circles show means. ***, $P < 0.001$; *, $P < 0.05$.